

Energy transfer efficiency in the FMO complex strongly coupled to a vibronic mode

Lev G. Mourokh¹ and Franco Nori^{2,3}

¹ *Department of Physics, Queens College,*

The City University of New York,

Flushing, New York 11367, USA

² *CEMS, RIKEN,*

Saitama, 351-0198, Japan

³ *Physics Department,*

The University of Michigan,

Ann Arbor, MI 48109-1040, USA

(Dated: October 9, 2018)

Abstract

Using methods of condensed matter and statistical physics, we examine the transport of excitons through the Fenna-Matthews-Olson (FMO) complex from a receiving antenna to a reaction center. Writing the equations of motion for the exciton creation/annihilation operators, we are able to describe the exciton dynamics, even in the regime when the reorganization energy is of the order of the intra-system couplings. In particular, we obtain the well-known quantum oscillations of the site populations. We determine the exciton transfer efficiency in the presence of a quenching field and protein environment. While the majority of the protein vibronic modes are treated as a heat bath, we address the situation when specific modes are strongly coupled to excitons and examine the effects of these modes on the quantum oscillations and the energy transfer efficiency. We find that, for the vibronic frequencies below 16 meV, the exciton transfer is drastically suppressed. We attribute this effect to the formation of “polaronic states” where the exciton is transferred back and forth between the two pigments with the absorption/emission of the vibronic quanta, instead of proceeding to the reaction center. The same effect suppresses the quantum beating at the vibronic frequency of 25 meV. We also show that the efficiency of the energy transfer can be enhanced when the vibronic mode strongly couples to the third pigment only, instead of coupling to the entire system.

I. INTRODUCTION

The effective energy transfer in photosynthetic complexes has been one of the focal points of experimental and theoretical studies during recent years [1, 2]. The light energy is absorbed by the pigments in the antenna systems and subsequently transferred to a reaction center, where the created electron-hole pairs are separated and the energy is converted to chemical compounds. The energy conversion efficiency of this process can reach 99% [3, 4]. The chromophore complexes located between the antenna and the reaction center are of special interest, because of the recent observation of the long-lived quantum coherence in the Fenna-Matthews-Olson (FMO) complex of green sulfur bacteria [5, 6] and marine cryptophyte algae [7, 8].

The FMO complex [9] is one of the most studied photosynthesis-related systems. It is a trimer with each unit consisting of seven bacteriochlorophyll a (BChl-a) molecules and with three more BChls between the units (so-called the eighth BChls). This molecular system is placed between an antenna and the reaction center where the charges are separated. The light harvested in the antenna excites one of the BChls and this excitation propagates through the complex until it reaches the reaction center. This energy transfer has been addressed in numerous theoretical works [10–28] employing various types of approximations. BChls are coupled to the protein environment and its role in the excitation transfer has been widely discussed. In particular, it was suggested that the interaction with the environment can assist exciton transport [29–34] and, moreover, can lead to a new type of excitonic-vibrational coherence [35–38]. However, it is still open question how this type of coherence affects the efficiency of the exciton transfer through the chromophore network.

In this paper, we examine the exciton propagation through the system of many inter-coupled chromophores to the reaction center in the presence of an external excitation, radiation heat bath, quenching field, and protein environment considered as a system of independent oscillators. The main focus here is to the coupling to a specific vibronic mode which cannot be treated as a heat bath. The coupling strengths of all the surrounding components are very different, so various levels of approximations should be used. In particular, the contributions of the quenching and radiation fields, as well as that of the reaction center, are calculated perturbatively within the secular approximation. The reorganization energy of the protein environment is of the order of the inter-chromophore couplings, so we have

to incorporate non-Markovian effects. However, in the case of slow protein motion and high enough temperatures, the dynamics under the time integral can be simplified. We do not apply this approximation for the strongly-coupled vibronic mode and also take into account the interplay of the last two processes. For all the above interactions, we take into account the contributions of both diagonal and off-diagonal elements of the density matrix.

The couplings of the system to the external light source and to a reaction center are explicitly included in our Hamiltonian. Therefore, we are able to calculate the rate of energy transfer to the reaction center and the rate of the energy absorption by the system and, correspondingly, to *directly* determine the efficiency of the energy transfer. Previously, [39, 40], the efficiency was calculated indirectly by the population of the last chromophore in the chain. It should be also emphasized that our approach is not restricted to the single-exciton-propagation case, and the chromophore network can contain as many excitons as the number of chromophores. Equations obtained for the general case are applied to the FMO complex. We show that for certain frequencies of the vibronic mode, the energy transfer is strongly suppressed. To explain these results, we determine the time dependencies of the chromophore populations and show that, for these frequencies, the excitation does not effectively reach the chromophore coupled to the reaction center, despite the fact that it has the lowest energy. We argue that this effect is the result of the excitonic-vibrational coherence [35–38], when the *polaronic mode* is formed and the excitation is transferred between two excitonic states with the emission/absorption of vibronic quanta, instead of proceeding to the reaction center. Eventually, the excitation energy is dissipated. The same effect can suppress the quantum beating which occurs in the populations of the first and second pigments. At a certain frequency of the vibronic mode, the polaronic mode forms between the first and sixth pigments and the exciton is transferred to the sixth chromophore instead of the second one. However, if the vibronic mode is strongly coupled to a specific (third) pigment, the efficiency of the energy transfer is even enhanced.

The rest of the paper is structured as follows. Section II contains the Hamiltonian of the system. In Section III, we determine the density matrix and derive its equations of motion. The efficiency of the energy transfer is defined in Section IV. This approach is applied to the FMO complex in Section V, where we find the dependence of the energy transfer efficiency on the frequency of the vibronic mode strongly coupled to the system and calculate the time dependencies of the chromophores populations. Section VI contains the conclusions of our

work.

II. HAMILTONIAN

We start from the general description of the exciton transfer through a system of N chromophores when these are coupled to each other, and each one of them can be coupled to the light source, reaction center, quenching and blackbody radiation fields, as well as the protein environment. In addition, the interaction with a specific strong vibronic mode is included. The Hamiltonian of this system consists of the following components:

(i) Unperturbed part

$$H_0 = \sum_n \epsilon_n a_n^\dagger a_n + \sum_{m \neq n} V_{mn} a_m^\dagger a_n - \sum_n (F_n e^{i\omega_0 t} a_n + F_n^* e^{-i\omega_0 t} a_n^\dagger), \quad (1)$$

where a_n^\dagger and a_n are the creation and annihilation operators for the excitations of the n -th chromophore, E_n is the excitation energy, V_{mn} is the inter-chromophores energy transfer amplitude, and F_n and ω_0 are the coupling strengths and frequency of the external light, respectively. It should be noted that the total number of excitations in the system depends on the coupling to the light source and can be as many as the number of chromophores. However, each of them can only be single-populated.

(ii) Coupling to the reaction center

$$H_{\text{trap}} = - \sum_n \sum_k \left(g_{kn} b_k^\dagger a_n + g_{kn}^* a_n^\dagger b_k \right), \quad (2)$$

where b_k^\dagger and b_k are the creation and annihilation operators for the excitations at the reaction center having its own Hamiltonian

$$H_{\text{RC}} = \sum_k \epsilon_k b_k^\dagger b_k. \quad (3)$$

(iii) Interaction with the blackbody radiation and quenching fields

$$H_{\text{Rec}} = - \sum_n (Q_n a_n^\dagger + Q_n^* a_n), \quad (4)$$

where the operator

$$Q_n = d_n (\mathcal{E}_{\text{rad}} + \mathcal{E}_{\text{quen}}), \quad (5)$$

is proportional to the sum of the fields multiplied by the dipole moment d_n of the n -chromophore. The Hamiltonians of the radiation heat bath, H_{Rad} , and the quenching field, H_{quen} , describe the free evolution of these degrees of freedom.

(iv) Coupling to the protein environment

$$H_{\text{e-ph}} = - \sum_{j,n} C_{jn} m_j \omega_j^2 x_j a_n^\dagger a_n. \quad (6)$$

We describe the environment, having the Hamiltonian

$$H_{\text{env}} = \sum_j \left(\frac{p_j^2}{2m_j} + \frac{m_j \omega_j^2 x_j^2}{2} \right), \quad (7)$$

as a set of independent harmonic oscillators with the position (x_j) and momentum (p_j) operators. The j -th oscillator has a mass m_j and a frequency ω_j . Here C_{jn} are the coupling strengths of the j -th phonon mode and the exciton at the n -th site.

(v) Coupling to a specific vibronic mode

$$H_{\text{e-vib}} = - \sum_n C_n M \Omega^2 X a_n^\dagger a_n, \quad (8)$$

with the Hamiltonian

$$H_{\text{vib}} = \frac{P^2}{2M} + \frac{M \Omega^2 X^2}{2}, \quad (9)$$

involving the position X and momentum P operators. Here, M , Ω and C_n are the mass, frequency, and the coupling strengths, respectively, associated with this vibronic mode.

The time dependence of the unperturbed Hamiltonian, Eq. (1), can be removed by means of the unitary transformation,

$$U = \exp \left(-i \sum_m N_m \omega_0 t \right) = \prod_m \exp(-i N_m \omega_0 t), \quad (10)$$

where $N_m = a_m^\dagger a_m$. Accordingly, the total Hamiltonian has the form

$$\begin{aligned} H = & \sum_n (\epsilon_n - \omega_0) a_n^\dagger a_n + \sum_{m \neq n} V_{mn} a_m^\dagger a_n - \sum_n (F_n a_n + F_n^* a_n^\dagger) \\ & - \sum_n (e^{i\omega_0 t} Q_n a_n^\dagger + e^{-i\omega_0 t} Q_n^\dagger a_n) - \sum_{k,n} (e^{-i\omega_0 t} g_{kn} b_k^\dagger a_n + e^{i\omega_0 t} g_{kn}^* a_n^\dagger b_k) \\ & - \sum_{j,n} C_{jn} m_j \omega_j^2 x_j a_n^\dagger a_n - \sum_n C_n M \Omega^2 X a_n^\dagger a_n \\ & + H_{\text{env}} + H_{\text{vib}} + H_{\text{RC}} + H_{\text{Rad}} + H_{\text{quen}}. \end{aligned} \quad (11)$$

III. DENSITY MATRIX AND RATE EQUATIONS

The unperturbed Hamiltonian can be numerically diagonalized with the determination of its eigenenergies and eigenfunctions, as

$$H_0|\mu\rangle = E_\mu|\mu\rangle. \quad (12)$$

Accordingly, we can construct the density matrix in the form

$$\rho_{\mu\nu} = |\mu\rangle\langle\nu|, \quad (13)$$

and express all operators in terms of this matrix. In particular, the exciton operators are given by

$$a_m = \sum_{\mu\nu} a_{m;\mu\nu} \rho_{\mu\nu} = \sum_{\mu\nu} \langle\mu|a_m|\nu\rangle \rho_{\mu\nu}, \quad N_m = a_m^\dagger a_m = \sum_{\mu\nu} \langle\mu|N_m|\nu\rangle \rho_{\mu\nu}. \quad (14)$$

Correspondingly, the total Hamiltonian of the system can be written as

$$H = H_0 - \sum_{\mu\nu} \mathcal{A}_{\mu\nu} \rho_{\mu\nu}, \quad (15)$$

where $\mathcal{A}_{\mu\nu}$ includes contributions of all terms of Eq. (11) not involved in H_0 . It should be noted that the external light source is already included in H_0 and the basic states are determined accordingly.

We treat the density matrix elements $\rho_{\mu\nu}$ as Heisenberg operators and the corresponding equations of motion are given by

$$i\dot{\rho}_{\mu\nu} = [\rho_{\mu\nu}, H]_- = -\omega_{\mu\nu} \rho_{\mu\nu} - \sum_{\alpha} (\mathcal{A}_{\nu\alpha} \rho_{\mu\alpha} - \mathcal{A}_{\alpha\mu} \rho_{\alpha\nu}), \quad (16)$$

where $\omega_{\mu\nu} = E_\mu - E_\nu$.

To evaluate specific contributions to Eq. (16), we apply the approach introduced in Ref. [41] where the set of exact non-Markovian equations was derived. The coupling strengths of the chromophores to surrounding fields are different, and, correspondingly, various levels of approximations can be used. The details of the calculations are given in the Appendix.

The time evolution of the off-diagonal ($\mu \neq \nu$) elements of the exciton matrix $\langle\rho_{\mu\nu}\rangle(t)$ is given by

$$\rho_{\mu\nu}(t) = \exp[i\omega_{\mu\nu} t] \exp[-(\bar{\lambda}_{\mu\nu}^{\text{ph}} + \bar{\lambda}_{\mu\nu}^{\text{vib}}) T t^2] \exp[-\Gamma_{\mu\nu} t] \rho_{\mu\nu}(0), \quad (17)$$

where $\bar{\lambda}_{\mu\nu}^{\text{ph}}$ and $\bar{\lambda}_{\mu\nu}^{\text{vib}}$ are the reorganization energies associated with the phonon heat bath and the strongly-coupled vibronic mode, respectively; and the dephasing rate

$$\Gamma_{\mu\nu} = \Gamma_{\mu\nu}^{\text{ph}} + \Gamma_{\mu\nu}^{\text{vib}} + \Gamma_{\mu\nu}^{\text{rec}} + \Gamma_{\mu\nu}^{\text{trap}}, \quad (18)$$

includes contributions of all processes involved.

The exciton distribution $\langle \rho_\mu \rangle$ over the eigenstates $|\mu\rangle$ of the Hamiltonian H_0 evolves according to the equation

$$\langle \dot{\rho}_\mu \rangle + \gamma_\mu \langle \rho_\mu \rangle = \sum_\alpha \gamma_{\mu\alpha} \langle \rho_\alpha \rangle, \quad (19)$$

where the relaxation matrix $\gamma_{\mu\alpha}$ contains contributions, $\gamma_{\mu\alpha}^{\text{ph}}$ and $\gamma_{\mu\alpha}^{\text{vib}}$, of the non-diagonal environment and vibronic operators, as well as contributions of recombination, $\gamma_{\mu\alpha}^{\text{rec}}$, and trapping, $\gamma_{\mu\alpha}^{\text{trap}}$, processes, as

$$\gamma_{\mu\alpha} = \gamma_{\mu\alpha}^{\text{ph}} + \gamma_{\mu\alpha}^{\text{vib}} + \gamma_{\mu\alpha}^{\text{rec}} + \gamma_{\mu\alpha}^{\text{trap}}, \quad (20)$$

The density relaxation rate is given by

$$\gamma_\mu = \sum_\alpha \gamma_{\alpha\mu}. \quad (21)$$

The steady-state exciton distribution ρ_μ^0 can be found from the equation

$$\gamma_\mu \rho_\mu^0 = \sum_\alpha \gamma_{\mu\alpha} \rho_\alpha^0, \quad (22)$$

taking into account the normalization condition $\sum_\mu \rho_\mu^0 = 1$.

IV. ENERGY-TRANSFER EFFICIENCY

We define the energy-transfer efficiency as a ratio of the average rate of the energy transmission going to the reaction center to the total rate of electromagnetic energy absorption by the system. The first quantity is given by

$$\mathcal{W}_{\text{RC}} = \frac{d}{dt} E_{\text{RC}} = \sum_k \epsilon_k \langle \dot{N}_k \rangle, \quad (23)$$

where $N_k = b_k^\dagger b_k$. The interaction of the system with the monochromatic light source can be rewritten in terms of the electric field strength, $\mathcal{E}_n(t) = F_n e^{i\omega_0 t} + H.c.$, and the polarization

$\mathcal{P}_n = a_n^\dagger + a_n$, as $H_F = -\sum_n \mathcal{E}_n(t) \mathcal{P}_n$. Thus, the rate of the light energy absorption has the form

$$\mathcal{W} = -\sum_n \langle \mathcal{P}_n \dot{\mathcal{E}}_n(t) \rangle \simeq -i\omega_0 \sum_n \langle F_n e^{i\omega_0 t} a_n - F_n^* e^{-i\omega_0 t} a_n^\dagger \rangle. \quad (24)$$

This energy can be determined using the equation of motion for the operator of the total number of excitations, $\sum_m N_m$, and can be written in the form of the balance relation:

$$\mathcal{W} = \mathcal{W}_m + \mathcal{W}_k + \mathcal{W}_{\text{Rec}} = \omega_0 \sum_m \langle \dot{N}_m \rangle + \omega_0 \sum_k \langle \dot{N}_k \rangle + i\omega_0 \sum_m \langle e^{-i\omega_0 t} Q_m^\dagger a_m - e^{i\omega_0 t} a_m^\dagger Q_m \rangle. \quad (25)$$

Correspondingly, the energy transfer efficiency is given by

$$\eta = \mathcal{W}_{\text{RC}}/\mathcal{W}. \quad (26)$$

For the steady state, the total number of excitons in the system is constant, so $\mathcal{W}_m = 0$. \mathcal{W}_{RC} , \mathcal{W}_k , and \mathcal{W}_{Rec} can be calculated similar to the relaxation rates of Appendix and they have forms

$$\mathcal{W}_{\text{RC}} = \sum_n \sum_{\mu\nu} (\omega_0 - \omega_{\mu\nu}) |a_{n;\mu\nu}|^2 \times \{ \Gamma_n^{\text{trap}}(\omega_0 + \omega_{\mu\nu}) [1 + n(\omega_0 + \omega_{\mu\nu})] \langle \rho_\nu^0 \rangle - \Gamma_n^{\text{trap}}(\omega_0 - \omega_{\mu\nu}) n(\omega_0 - \omega_{\mu\nu}) \langle \rho_\mu^0 \rangle \}, \quad (27)$$

$$\mathcal{W}_k = \omega_0 \sum_n \sum_{\mu\nu} |a_{n;\mu\nu}|^2 \times \{ \Gamma_n^{\text{trap}}(\omega_0 + \omega_{\mu\nu}) [1 + n(\omega_0 + \omega_{\mu\nu})] \langle \rho_\nu^0 \rangle - \Gamma_n^{\text{trap}}(\omega_0 - \omega_{\mu\nu}) n(\omega_0 - \omega_{\mu\nu}) \langle \rho_\mu^0 \rangle \}, \quad (28)$$

and

$$\mathcal{W}_{\text{Rec}} = 2\omega_0 \sum_n \sum_{\mu\nu} |a_{n;\mu\nu}|^2 \times \{ \chi_n''(\omega_0 + \omega_{\mu\nu}) [1 + n(\omega_0 - \omega_{\mu\nu})] \langle \rho_\nu^0 \rangle - \chi_n''(\omega_0 - \omega_{\mu\nu}) n(\omega_0 - \omega_{\mu\nu}) \langle \rho_\mu^0 \rangle \}. \quad (29)$$

V. FMO COMPLEX

In this Section, we apply the equations obtained above to a specific system, FMO complex containing seven pigments. We assume that the external light creates the exciton in the Bchl 1 and the reaction center is coupled to the Bchl 3. We ignore the eighth Bchl [42] in this work because its role in the energy transfer is not clear yet. In the absence of an external

light source, the energies of the seven exciton sites with respect to the lowest one and the transfer matrix elements (in meV) are given by [43]

$$E_n + V_{mn} = \begin{pmatrix} 29.76 & -10.87 & 0.68 & -0.73 & 0.83 & -1.7 & -1.23 \\ -10.87 & 39.06 & 3.73 & 1.02 & 0.09 & 1.46 & 0.53 \\ 0.68 & 3.73 & 0 & -6.63 & -0.27 & -1.19 & 0.74 \\ -0.73 & 1.02 & -6.63 & 16.12 & -8.77 & -2.11 & -7.85 \\ 0.83 & 0.09 & -0.27 & -8.77 & 35.34 & 10.06 & -0.16 \\ -1.7 & 1.46 & -1.19 & -2.11 & 10.06 & 53.94 & 4.92 \\ -1.23 & 0.53 & 0.74 & -7.85 & -0.16 & 4.92 & 30.38 \end{pmatrix} \quad (30)$$

In our model, each Bchl can be populated, so we have a total of 128 ($=2^7$) basic states. The energies of the first 64 states (solutions of Eq. (12)) are shown in Fig. 1 jointly with the bare energies of the pigments. It is evident from this figure that the lowest state is separated from the upper states by energy gap of approximately 13 meV.

To determine the energy transfer efficiency, the spectral functions of the environment should be defined. We use the Drude-Gaussian form of the spectral function for the heat bath modes, as

$$J^{\text{ph}}(\omega) = \lambda^{\text{ph}} \left(\frac{\omega}{\omega_c} \right) \exp \left(-\frac{\omega}{\omega_c} \right). \quad (31)$$

This type of spectral function is used both for the description of the environment in photosynthetic complexes [44] and for general condensed matter problems [45]. The spectral function for the specific vibronic mode is given by

$$J^{\text{vib}}(\omega) = \lambda^{\text{vib}} \Omega \delta(\omega - \Omega). \quad (32)$$

The total spectral function, including the contributions of the heat bath modes and a specific vibronic mode, is shown in Fig. 2. The cutting frequency ω_c is taken to be 18.6 meV and the frequency of the vibronic mode is chosen to be 10 meV for this figure.

The efficiency, Eq. (26), is shown in Fig. 3 as a function of the frequency of the vibronic mode. One can see that with decreasing frequency, the efficiency starts to drop at approximately 16 meV. This drop can be quite significant, up to 4 times at low frequencies. We also show in this figure the efficiency value for case when there is no strong coupling to the specific vibronic mode which equals to 0.8314 for our set of parameters. For our calculations, we use: the temperature $T = 77$ K, the light-Bchl coupling strength $F = 10^{-4}$ meV

(with the light coupled to the first pigment only), refraction index $n_{\text{refr}} = 1.42$, the heat bath reorganization energy $\lambda^{\text{ph}} = 4.34$ meV, the reorganization energy of the vibronic mode $\lambda^{\text{vib}} = 18.6$ meV, coupling to the reaction center $g_{nk} = 6.6 \cdot 10^{-3}$ meV (with only the third pigment coupled), and the coupling to the quenching field $Q_m = 6.6 \cdot 10^{-4}$ meV.

To understand the physical reasons for such significant drop of the energy transfer efficiency, we calculate the time dependence of the pigment populations with the results shown in Fig. 4(a-f). For initial conditions, we use the situation when the first pigment (coupled to the light) is populated and all other Bchls are not. With no strong coupling to the vibronic mode (Fig. 4a), there are well-known quantum oscillations of populations of the first and second pigments (for times of about 0.5 ps) and by the time of about 3 ps the exciton energy is mostly transferred to the third pigment coupled to the reaction center. It should be noted that the fifth, sixth, and seventh pigments remain unpopulated all the time. Almost the same picture can be seen for the high frequency of the vibronic mode (Fig. 4f). With the frequency decreasing, the fifth, sixth, and seventh pigments start to be populated and at $\Omega = 4$ meV all seven Bchls are populated almost equally by 3 ps. It should be emphasized that the energies of the Bchl 3 and Bchl 4, Bchl 4 and Bchl 5, and Bchl 5 and Bchl 6, are all separated by 16-19 meV. Accordingly, the strong coupling to the vibronic modes of appropriate frequency with the preservation of “vibronic coherence” [35–37] can lead to the formation of “polaronic modes” between corresponding pigments. As the coupling to the vibronic mode is strong, multi-phonon interaction is possible. Formally, it corresponds to non-vanishing contributions of the high-order Bessel functions of Eqs. (A15) and (A16). Moreover, one can see from these equations that the interference between the specific mode and heat bath modes is possible, therefore the energy mismatch preventing the polaronic mode formation can be compensated by the heat bath. As a result, the exciton, which is transferred to Bchl 3 from Bchl 2, does not proceed to the reaction center, but oscillates between Bchls 3, 4 5, and 6 and the energy is eventually lost to the quenching field or the heat bath.

Of special interest is the suppression of the quantum beating between Bchl 1 and Bchl 2 at $\Omega = 25$ meV, Fig. 4e. It can be a result of similar polaronic mode formation. The separation between the energies of Bchl 1 and Bchl 6 is about 24 meV, so vibronic-assisted transfer between these pigments is possible. Correspondingly, the exciton proceeds to the third pigment not via Bchl 2 but via Bchls 6, 5, and 4. It should be noted that the energy

efficiency is *not* suppressed at this frequency.

Our approach allows us to examine the situation when the vibronic mode is deliberately coupled to a specific pigment. In Fig. 5, we show the energy transfer efficiency as a function of the vibronic mode frequency, when only the Bchl 3 is coupled to the vibronic mode. One can see that the efficiency is suppressed at low frequencies but not as drastically as in Fig. 3. The reason for such relatively small suppression is that the polaronic mode is formed between the Bchl 3 and Bchl 4 only, with no exciton transfer farther to Bchls 5 and 6. However, it is evident from Fig. 5 that at $\Omega = 30$ meV, the energy transfer efficiency even exceeds the value for no coupling to the vibronic mode. The corresponding time dependencies of the pigment populations are shown in Fig. 6. For $\Omega = 4$ meV, Fig. 6a, Bchls 5 and 6 remain unpopulated, in contrast to Fig. 4b, when all the sites are coupled to the vibronic mode. One can see from Fig. 6b that for $\Omega = 30$ meV the population of Bchl 3 at 3 ps is even higher than that of the unperturbed system, Fig. 4a.

VI. CONCLUSIONS

In conclusion, we have developed an approach allowing to study the exciton transfer through a network for the case when the reorganization energy is of the order of the inter-site couplings. Our method is not restricted to the one-particle case, so we can describe the propagation of several excitons through the system. We have taken into account the effects of radiative and quenching baths, as well as the coupling to the reaction center, perturbatively with the secular approximation. We have gone beyond this approximation for the protein environment examining the non-Markovian effects as well. While the majority vibronic modes have been treated as a heat bath, we have also included the strong coupling to a specific vibronic mode into consideration. For the heat bath modes, we have used a high temperature (or low frequency) approximation for the dynamics inside the non-Markovian integral, while the specific mode was treated exactly. Accordingly, we have determined the contributions of multi-phonon processes and obtained that the contributions of the heat bath modes and the vibronic mode are interconnected, as the frequency and the reorganization energy of the vibronic mode is involved in the relaxation matrix for the heat bath and vice versa.

We have obtained the efficiency of the energy transfer directly, as the ratio of the en-

ergy transferred to the reaction center and the total energy absorbed by the system. We have calculated this efficiency for a specific system, the FMO complex, and found that this efficiency is dropped significantly, if the energy of the strongly-coupled vibronic mode becomes smaller than 16 meV. We have attributed that to the formation of “polaronic modes” where the exciton is transferred back and forth between two pigments with absorption and emission of vibronic quanta. Accordingly, the exciton instead of proceeding to the reaction center from the lowest-energy Bchl 3, is transferred sequentially to Bchls 4, 5, and 6, and the energy is eventually lost to the quenching field or to the environment heat bath. We have illustrated this effect determining the time dependencies of the pigment populations and showing that for the low frequency of the strongly-coupled vibronic mode, the exciton is almost equally distributed between all the pigments. We have obtained the well-known oscillations in the populations of Bchl 1 and Bchl 2 and showed that these oscillations are suppressed at the vibronic mode frequency of 30 meV. This corresponds to the separation of the energies of Bchls 1 and 6 and we attribute this effect to the polaronic mode between these pigments and the energy transfer avoiding Bchl 2. It is interesting that it does not affect the energy transfer efficiency. We have also shown that the efficiency can even be enhanced if the specific vibronic mode is coupled deliberately to Bchl 3. In this case, the obtained value exceeds that for the unperturbed complex.

Appendix A: Contributions of various mechanisms to the evolution of the density matrix

In the Appendix, we provide the calculations of various contributions to the equation of the motion for the density matrix, Eq. (16). The chromophore sites are weakly coupled to the radiative and quenching bath, as well to the reaction center. Hence, the contribution of these components of the variable \mathcal{A} to the Eq. (16) can be treated perturbatively with the secular approximation. Thus, for the diagonal part, $\rho_\mu = \rho_{\mu\mu} = |\mu\rangle\langle\mu|$, of the operator $\rho_{\mu\nu}$ we obtain

$$-i\langle[\rho_\mu, H_{\text{rec}} + H_{\text{trap}}]_-\rangle = -\sum_{\alpha}(\gamma_{\alpha\mu}^{\text{rec}} + \gamma_{\alpha\mu}^{\text{trap}})\langle\rho_\mu\rangle + \sum_{\alpha}(\gamma_{\mu\alpha}^{\text{rec}} + \gamma_{\mu\alpha}^{\text{trap}})\langle\rho_\alpha\rangle. \quad (\text{A1})$$

Recombination events and the trapping of excitations by the reaction center provide the following contribution to the dephasing of excitonic degrees of freedom ($\mu \neq \nu$)

$$-i\langle[\rho_{\mu\nu}, H_{\text{rec}} + H_{\text{trap}}]_-\rangle = -(\Gamma_{\mu\nu}^{\text{rec}} + \Gamma_{\mu\nu}^{\text{trap}})\langle\rho_{\mu\nu}\rangle. \quad (\text{A2})$$

The relaxation rates are given by

$$\begin{aligned} \gamma_{\mu\alpha}^{\text{rec}} = & 2 \sum_n |a_{n;\alpha\mu}|^2 \chi_n''(\omega_0 + \omega_{\mu\alpha}) n(\omega_0 + \omega_{\mu\alpha}) + \\ & 2 \sum_n |a_{n;\mu\alpha}|^2 \chi_n''(\omega_0 - \omega_{\mu\alpha}) [1 + n(\omega_0 - \omega_{\mu\alpha})] \end{aligned} \quad (\text{A3})$$

and

$$\begin{aligned} \gamma_{\mu\alpha}^{\text{trap}} = & \sum_n |a_{n;\alpha\mu}|^2 \Gamma_n^{\text{trap}}(\omega_0 + \omega_{\mu\alpha}) n(\omega_0 + \omega_{\mu\alpha}) + \\ & \sum_n |a_{n;\mu\alpha}|^2 \Gamma_n^{\text{trap}}(\omega_0 - \omega_{\mu\alpha}) [1 + n(\omega_0 - \omega_{\mu\alpha})]. \end{aligned} \quad (\text{A4})$$

The dephasing rates consist of two parts, $\Gamma_{\mu\nu}^{\text{rec}} = \Gamma_{\mu}^{\text{rec}} + \Gamma_{\nu}^{\text{rec}}$, and $\Gamma_{\mu\nu}^{\text{trap}} = \Gamma_{\mu}^{\text{trap}} + \Gamma_{\nu}^{\text{trap}}$, where

$$\begin{aligned} \Gamma_{\mu}^{\text{rec}} = & \sum_{n\alpha} |a_{n;\mu\alpha}|^2 \chi_n''(\omega_0 - \omega_{\mu\alpha}) n(\omega_0 - \omega_{\mu\alpha}) + \\ & \sum_{n\alpha} |a_{n;\alpha\mu}|^2 \chi_n''(\omega_0 + \omega_{\mu\alpha}) [1 + n(\omega_0 + \omega_{\mu\alpha})], \end{aligned} \quad (\text{A5})$$

and

$$\begin{aligned} \Gamma_{\mu}^{\text{trap}} = & (1/2) \sum_{n\alpha} |a_{n;\mu\alpha}|^2 \Gamma_n^{\text{trap}}(\omega_0 - \omega_{\mu\alpha}) n(\omega_0 - \omega_{\mu\alpha}) + \\ & (1/2) \sum_{n\alpha} |a_{n;\alpha\mu}|^2 \Gamma_n^{\text{trap}}(\omega_0 + \omega_{\mu\alpha}) [1 + n(\omega_0 + \omega_{\mu\alpha})]. \end{aligned} \quad (\text{A6})$$

In this expressions, $n(\omega) = [\exp(\omega/T) - 1]^{-1}$ is the Bose distribution, Γ_n^{trap} is the trapping rate defined as

$$\Gamma_n^{\text{trap}} = 2\pi \sum_k |g_{kn}|^2 \delta(\omega - \epsilon_k), \quad (\text{A7})$$

and the imaginary part of the bath susceptibility, $\chi_n''(\omega)$, contains contributions of the black-body heat bath and the Ohmic quenching bath, as

$$\chi_n''(\omega) = (2/3)n_{\text{refr}}|d_n|^2(\omega/c)^3 + \alpha_n\omega, \quad (\text{A8})$$

with n_{refr} being the refractive index of the medium.

The interaction with the protein environment cannot be considered weak, and, correspondingly, we cannot use the secular approximation employed in the previous subsection. Following Ref. [41], we introduce various spectral densities and reorganization energies as

$$\begin{aligned}
J_\mu^{\text{ph}}(\omega) &= \sum_j \frac{m_j \omega_j^3}{2} \left(\sum_m C_{jm} \langle \mu | N_m | \mu \rangle \right)^2 \delta(\omega - \omega_j), \\
\bar{J}_{\mu\nu}^{\text{ph}}(\omega) &= \sum_j \frac{m_j \omega_j^3}{2} \left(\sum_m C_{jm} \langle \mu | N_m | \mu \rangle - \sum_m C_{jm} \langle \nu | N_m | \nu \rangle \right)^2 \delta(\omega - \omega_j) \\
\tilde{J}_{\mu\nu}^{\text{ph}}(\omega) &= \sum_j \frac{m_j \omega_j^3}{2} \left| \sum_m C_{jm} \langle \mu | N_m | \nu \rangle \right|^2 \delta(\omega - \omega_j), \mu \neq \nu,
\end{aligned} \tag{A9}$$

$$\begin{aligned}
\lambda_\mu^{\text{ph}} &= \int_0^\infty \frac{d\omega}{\omega} J_\mu^{\text{ph}}(\omega) = \sum_j \frac{m_j \omega_j^2}{2} \left(\sum_m C_{jm} \langle \mu | N_m | \mu \rangle \right)^2, \\
\bar{\lambda}_{\mu\nu}^{\text{ph}} &= \int_0^\infty \frac{d\omega}{\omega} \bar{J}_{\mu\nu}^{\text{ph}}(\omega) = \sum_j \frac{m_j \omega_j^2}{2} \left(\sum_m C_{jm} \langle \mu | N_m | \mu \rangle - \sum_m C_{jm} \langle \nu | N_m | \nu \rangle \right)^2,
\end{aligned} \tag{A10}$$

and

$$\begin{aligned}
\lambda_\mu^{\text{vib}} &= \frac{M\Omega^2}{2} \left(\sum_m C_m \langle \mu | N_m | \mu \rangle \right)^2, \\
\bar{\lambda}_{\mu\nu}^{\text{vib}} &= \frac{M\Omega^2}{2} \left(\sum_m C_m \langle \mu | N_m | \mu \rangle - \sum_m C_m \langle \nu | N_m | \nu \rangle \right)^2, \\
\tilde{\lambda}_{\mu\nu}^{\text{vib}} &= \frac{M\Omega^2}{2} \left| \sum_m C_m \langle \mu | N_m | \nu \rangle \right|^2, \mu \neq \nu.
\end{aligned} \tag{A11}$$

It was shown in Ref. [41] that the contribution of diagonal environment fluctuations can be determined exactly and they affect the off-diagonal elements of the density matrix only. With inclusion of an additional vibronic mode, the time evolution caused by these diagonal fluctuations has the form

$$\rho_{\mu\nu}(t) = \exp[i\omega_{\mu\nu} t] \exp[-(\bar{\lambda}_{\mu\nu}^{\text{ph}} + \bar{\lambda}_{\mu\nu}^{\text{vib}}) T t^2] \rho_{\mu\nu}(0). \tag{A12}$$

We evaluate the internal dynamics in the non-Markovian integrals and obtain the following contributions of non-diagonal environment and vibronic fluctuations to Eq. (16). (It should be noted that high temperature and low environment frequencies approximations of

Ref. [41] have been applied to the heat bath contribution, not to that of the specific single mode.) The evolution of the diagonal matrix elements is given by

$$\langle -i[\rho_\mu, H_{e\text{-ph}} + H_{e\text{-vib}}]_- \rangle = - \sum_\alpha (\gamma_{\alpha\mu}^{\text{ph}} + \gamma_{\alpha\mu}^{\text{vib}}) \langle \rho_\mu \rangle + \sum_\alpha (\gamma_{\mu\alpha}^{\text{ph}} + \gamma_{\mu\alpha}^{\text{vib}}) \langle \rho_\alpha \rangle. \quad (\text{A13})$$

For the off-diagonal elements, we obtain

$$\langle -i[\rho_{\mu\nu}, H_{e\text{-ph}} + H_{e\text{-vib}}]_- \rangle = -(\Gamma_{\mu\nu}^{\text{ph}} + \Gamma_{\mu\nu}^{\text{vib}}) \langle \rho_{\mu\nu} \rangle. \quad (\text{A14})$$

The relaxation matrices are given by

$$\begin{aligned} \gamma_{\mu\alpha}^{\text{ph}} = & \sqrt{\frac{\pi}{\bar{\lambda}_{\alpha\mu}^{\text{ph}} T}} \exp \left[-\frac{\bar{\lambda}_{\mu\alpha}^{\text{vib}}}{\Omega} \coth \frac{\Omega}{2T} \right] \sum_{l=-\infty}^{\infty} J_l \left[\frac{\bar{\lambda}_{\mu\alpha}^{\text{vib}}}{\Omega} \right] \int_0^\infty d\omega \tilde{J}_{\alpha\mu}^{\text{ph}}(\omega) n(\omega) \\ & \times \left(I_0 \left[\frac{\bar{\lambda}_{\mu\alpha}^{\text{vib}}}{\Omega} \coth \frac{\Omega}{2T} \right] \left(\exp \left[-\frac{(\omega + \Omega_{\alpha\mu} + l\Omega - \bar{\lambda}_{\alpha\mu}^{\text{ph}})^2}{4\bar{\lambda}_{\alpha\mu}^{\text{ph}} T} \right] \right. \right. \\ & \quad \left. \left. + \exp \left(\frac{\omega}{T} \right) \exp \left[-\frac{(\omega - \Omega_{\alpha\mu} - l\Omega + \bar{\lambda}_{\alpha\mu}^{\text{ph}})^2}{4\bar{\lambda}_{\alpha\mu}^{\text{ph}} T} \right] \right) \right. \\ & + \sum_{s=1}^{\infty} I_s \left[\frac{\bar{\lambda}_{\mu\alpha}^{\text{vib}}}{\Omega} \coth \frac{\Omega}{2T} \right] \left\{ \exp \left[-\frac{(\omega + \Omega_{\alpha\mu} + (l+s)\Omega - \bar{\lambda}_{\alpha\mu}^{\text{ph}})^2}{4\bar{\lambda}_{\alpha\mu}^{\text{ph}} T} \right] \right. \\ & \quad \left. + \exp \left[-\frac{(\omega + \Omega_{\alpha\mu} + (l-s)\Omega - \bar{\lambda}_{\alpha\mu}^{\text{ph}})^2}{4\bar{\lambda}_{\alpha\mu}^{\text{ph}} T} \right] \right. \\ & \quad \left. + \exp \left(\frac{\omega}{T} \right) \left(\exp \left[-\frac{(\omega + \Omega_{\alpha\mu} + (l+s)\Omega - \bar{\lambda}_{\alpha\mu}^{\text{ph}})^2}{4\bar{\lambda}_{\alpha\mu}^{\text{ph}} T} \right] \right. \right. \\ & \quad \left. \left. + \exp \left[-\frac{(\omega + \Omega_{\alpha\mu} + (l-s)\Omega - \bar{\lambda}_{\alpha\mu}^{\text{ph}})^2}{4\bar{\lambda}_{\alpha\mu}^{\text{ph}} T} \right] \right) \right\} \left. \right) \end{aligned} \quad (\text{A15})$$

and

$$\begin{aligned}
\gamma_{\mu\alpha}^{\text{vib}} = & \sqrt{\frac{\pi}{\bar{\lambda}_{\alpha\mu}^{\text{ph}} T}} \exp \left[-\frac{\bar{\lambda}_{\mu\alpha}^{\text{vib}}}{\Omega} \coth \frac{\Omega}{2T} \right] \sum_{l=-\infty}^{\infty} J_l \left[\frac{\bar{\lambda}_{\mu\alpha}^{\text{vib}}}{\Omega} \right] \Omega \tilde{\lambda}_{\alpha\mu}^{\text{vib}} n(\Omega) \\
& \times \left(I_0 \left[\frac{\bar{\lambda}_{\mu\alpha}^{\text{vib}}}{\Omega} \coth \frac{\Omega}{2T} \right] \left(\exp \left[-\frac{(\Omega + \Omega_{\alpha\mu} + l\Omega - \bar{\lambda}_{\alpha\mu}^{\text{ph}})^2}{4\bar{\lambda}_{\alpha\mu}^{\text{ph}} T} \right] \right. \right. \\
& \quad \left. \left. + \exp \left(\frac{\Omega}{T} \right) \exp \left[-\frac{(\Omega - \Omega_{\alpha\mu} - l\Omega + \bar{\lambda}_{\alpha\mu}^{\text{ph}})^2}{4\bar{\lambda}_{\alpha\mu}^{\text{ph}} T} \right] \right) \right. \\
& + \sum_{s=1}^{\infty} I_s \left[\frac{\bar{\lambda}_{\mu\alpha}^{\text{vib}}}{\Omega} \coth \frac{\Omega}{2T} \right] \left\{ \exp \left[-\frac{(\Omega + \Omega_{\alpha\mu} + (l+s)\Omega - \bar{\lambda}_{\alpha\mu}^{\text{ph}})^2}{4\bar{\lambda}_{\alpha\mu}^{\text{ph}} T} \right] \right. \\
& \quad \left. + \exp \left[-\frac{(\Omega + \Omega_{\alpha\mu} + (l-s)\Omega - \bar{\lambda}_{\alpha\mu}^{\text{ph}})^2}{4\bar{\lambda}_{\alpha\mu}^{\text{ph}} T} \right] \right. \\
& \quad \left. + \exp \left(\frac{\Omega}{T} \right) \left(\exp \left[-\frac{(\Omega + \Omega_{\alpha\mu} + (l+s)\Omega - \bar{\lambda}_{\alpha\mu}^{\text{ph}})^2}{4\bar{\lambda}_{\alpha\mu}^{\text{ph}} T} \right] \right. \right. \\
& \quad \left. \left. + \exp \left[-\frac{(\Omega + \Omega_{\alpha\mu} + (l-s)\Omega - \bar{\lambda}_{\alpha\mu}^{\text{ph}})^2}{4\bar{\lambda}_{\alpha\mu}^{\text{ph}} T} \right] \right) \right\} \Bigg), \tag{A16}
\end{aligned}$$

where

$$\Omega_{\alpha\mu} = \omega_{\alpha\mu} + \bar{\lambda}_{\mu}^{\text{ph}} - \bar{\lambda}_{\alpha}^{\text{ph}} + \bar{\lambda}_{\mu}^{\text{vib}} - \bar{\lambda}_{\alpha}^{\text{vib}} \tag{A17}$$

and $J_l(z)$ and $I_s(z)$ are the ordinary and modified Bessel functions, respectively. It should be emphasized that the heat bath and vibronic contributions are interconnected, as the vibronic mode is involved in the expression for $\gamma_{\mu\alpha}^{\text{ph}}$ and vice versa.

Similar to Ref. [41], the dephasing rates can be expressed as

$$\begin{aligned}
\Gamma_{\mu\nu}^{\text{ph,vib}} &= \Gamma_{\mu}^{\text{ph,vib}} + \Gamma_{\nu}^{\text{ph,vib}}, \\
\Gamma_{\mu}^{\text{ph,vib}} &= \frac{1}{2} \sum_{\alpha} \gamma_{\alpha\mu}^{\text{ph,vib}}. \tag{A18}
\end{aligned}$$

Acknowledgements

This work is partially supported by the RIKEN iTHES Project, MURI Center for Dynamic Magneto-Optics, JSPS-RFBR contract no. 12-02-92100, Grant-in-Aid for Scientific

Research (S), MEXT Kakenhi on Quantum Cybernetics and the JSPS via its FIRST program. L. M. was also partially supported by PSC-CUNY award 65245-00 43.

- [1] G. D. Scholes, G. R. Fleming, A. Olaya-Castro, and R. van Grondelle, *Nature Chem.* **3**, 763 (2011).
- [2] N. Lambert, Y. N. Chen, Y. C. Cheng, C. M. Li, G. Y. Chen, and F. Nori, *Nature Phys.* **9**, 10 (2013).
- [3] H. van Amerongen, L. Valkunas, and R. van Grondelle, *Photosynthetic Excitons*, World Scientific, Singapore, 2000.
- [4] R. E. Blankenship, *Molecular Mechanisms of Photosynthesis*, Blackwell Scientific Publications, 2002.
- [5] G. S. Engel, T. R. Calhoun, E. L. Read, T.-K. Ahn, T. Mancal, Y.-C. Cheng, R. E. Blankenship, and G. R. Fleming, *Nature* **446**, 782 (2007).
- [6] G. Panitchayangkoon, D. Hayes, K. A. Fransted, J. R. Caram, E. Harel, J. Wen, R. E. Blankenship, and G. S. Engel, *Proc. Natl. Acad. Sci. USA* **107**, 12766 (2010).
- [7] E. Collini, C. Y. Wong, K. E. Wilk, P. M. C. Curmi, P. Brumer, and G. D. Scholes, *Nature* **463**, 644 (2010).
- [8] C. Y. Wong, R. M. Alvey, D. B. Turner, K. E. Wilk, D. A. Bryant, P. M. G. Curmi, R. J. Silbey, and G. D. Scholes, *Nature Chem.* **4**, 396 (2012).
- [9] R. E. Fenna, B. W. Matthews, *Nature* **258**, 573 (1975).
- [10] S. Jang, Y.-C. Cheng, D. R. Reichman, and J. D. Eaves, *J. Chem. Phys.* **129**, 101104 (2008).
- [11] T. Renger, *Photosynth. Res.* **102**, 471 (2009).
- [12] A. Ishizaki, and G. R. Fleming, *PNAS* **106**, 17255 (2009).
- [13] B. Palmieri, D. Abramavicius, and S. Mukamel, *J. Chem. Phys.* **130**, 204512 (2009).
- [14] J. Cao and R. J. Silbey, *J. Phys. Chem. A* **113**, 13825 (2009).
- [15] A. Ishizaki, and G. R. Fleming, *New J. Phys.* **12**, 055004 (2010).
- [16] S. Hoyer, M. Sarovar, and K. B. Whaley, *New J. Phys.* **12**, 065041 (2010).
- [17] F. Fassioli and A. Olaya-Castro, *New J. Phys.* **12**, 085006 (2010).
- [18] J. Wu, F. Liu, Y. Shen, J. Cao, and R. J. Silbey, *New J. Phys.* **12**, 105012 (2010).
- [19] P. Nalbach and M. Thorwart, *J. Chem. Phys.* **132**, 194111 (2010).

- [20] S. Jang, *J. Chem. Phys.* **135**, 034105 (2011).
- [21] P. Nalbach, D. Braun, and M. Thorwart, *Phys. Rev. E* **84**, 041926 (2011).
- [22] P. Nalbach, A. Ishizaki, G. R. Fleming, and M. Thorwart, *New J. Phys.* **13**, 063040 (2011).
- [23] G. Ritschel, J. Roden, W. T. Strunz, and A. Eisfeld, *New J. Phys.* **13**, 113034 (2011).
- [24] C. Olbrich, J. Strümpfer, K. Schulten, and U. Kleinekathöfer, *J. Phys. Chem. B* **115**, 758 (2011).
- [25] C. Olbrich, T. L. C. Jansen, J. Liebers, M. Aghtar, J. Strümpfer, K. Schulten, J. Knoester, and U. Kleinekathöfer, *J. Phys. Chem. B* **115**, 8609 (2011).
- [26] D. P. S. McCutcheon and A. Nazir, *J. Chem. Phys.* **135**, 114501 (2011).
- [27] A. Kolli, A. Nazir, and A. Olaya-Castro, *J. Chem. Phys.* **135**, 154112 (2011).
- [28] R. Alicki and W. Miklaszewski, *J. Chem. Phys.* **136**, 134103 (2012).
- [29] M. B. Plenio, and S. F. Huelga, *New J. Phys.* **10**, 113019 (2008).
- [30] M. Mohseni, P. Robentrost, S. Lloyd, and A. Aspuru-Guzik, *J. Chem. Phys.* **129**, 176106 (2008).
- [31] P. Robentrost, M. Mohseni, I. Kassal, S. Lloyd, and A. Aspuru-Guzik, *New J. Phys.* **11**, 033003 (2009).
- [32] J. Roden, G. Schulz, A. Eisfeld, and J. Briggs, *J. Chem. Phys.* **130**, 044909 (2009).
- [33] H. Hossein-Nejad, A. Olaya-Castro, and G. Scholes, *J. Chem. Phys.* **136**, 024112 (2012).
- [34] A. Kolli, E. J. O'Reilly, G. Scholes, and A. Olaya-Castro, *J. Chem. Phys.* **137**, 174109 (2012).
- [35] N. Christensson, H. F. Kauffmann, T. Pullerits, and T. Mančal, *J. Phys. Chem. B* **116**, 7449 (2012).
- [36] T. Mančal, N. Christensson, V. Lukeš, F. Milota, O. Bixner, H. F. Kauffmann, and J. Hauer, *J. Phys. Chem. Lett.* **3**, 1497 (2012).
- [37] A. W. Chin, J. Prior, R. Rosenbach, F. Caycedo-Soler, S. F. Huelga, and M. B. Plenio, *Nat. Phys.* **9**, 113 (2013).
- [38] V. Tiwari, W. K. Peters, and D. M. Jonas, *PNAS* **110**, 1203 (2013).
- [39] S. Jesenko and M. Žnidarič, *J. Chem. Phys.* **138**, 174103 (2013).
- [40] B. Witt and F. Mintert, arXiv:1305.6860 [quant-ph].
- [41] P. K. Ghosh, A. Yu. Smirnov, and F. Nori, *J. Chem. Phys.* **134**, 244103 (2011).
- [42] M. S. Am Busch, F. Müh, M. E. Madjet, and T. Renger, *J. Phys. Chem. Lett.* **2**, 93 (2011).
- [43] J. Adolphs and T. Renger, *Biophys. J.* **91**, 2778 (2006).

- [44] M. Cho, H. M. Vaswani, T. Brixner, J. Stenger, and G. R. Fleming, *J. Phys. Chem. B* **109**, 10542 (2005).
- [45] A. J. Leggett, S. Chakravarty, A. T. Dorsey, M. P. A. Fisher, A. Garg, and W. Zwerger, *Rev. Mod. Phys.* **59**, 1 (1987).

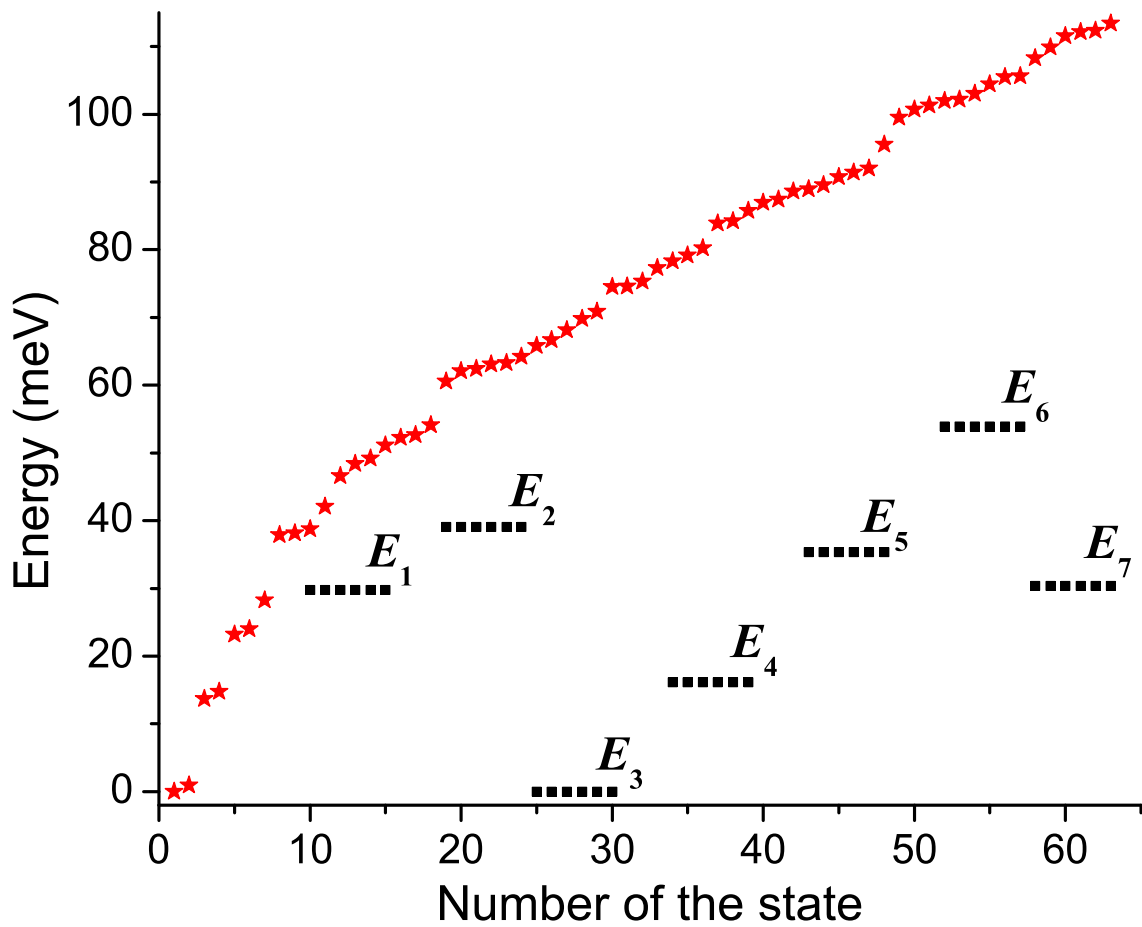


FIG. 1: (Color online) Eigenenergies (red stars) of the unperturbed Hamiltonian. The bare energies of the seven pigments of the FMO complex are shown as horizontal black dashed segments.

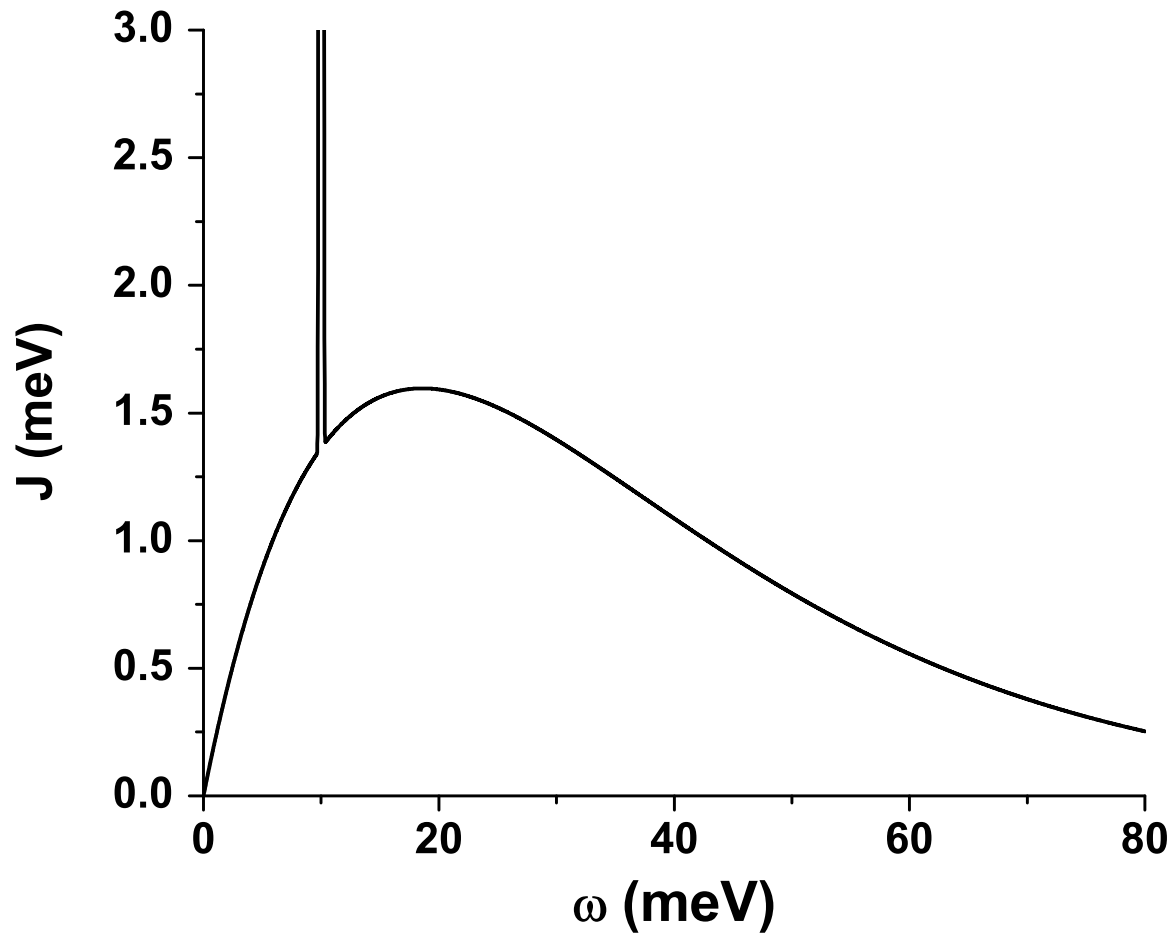


FIG. 2: (Color online) Environment spectral function $J(\omega)$ including contributions from the heat bath and a specific vibronic mode with frequency $\Omega = 10$ meV.

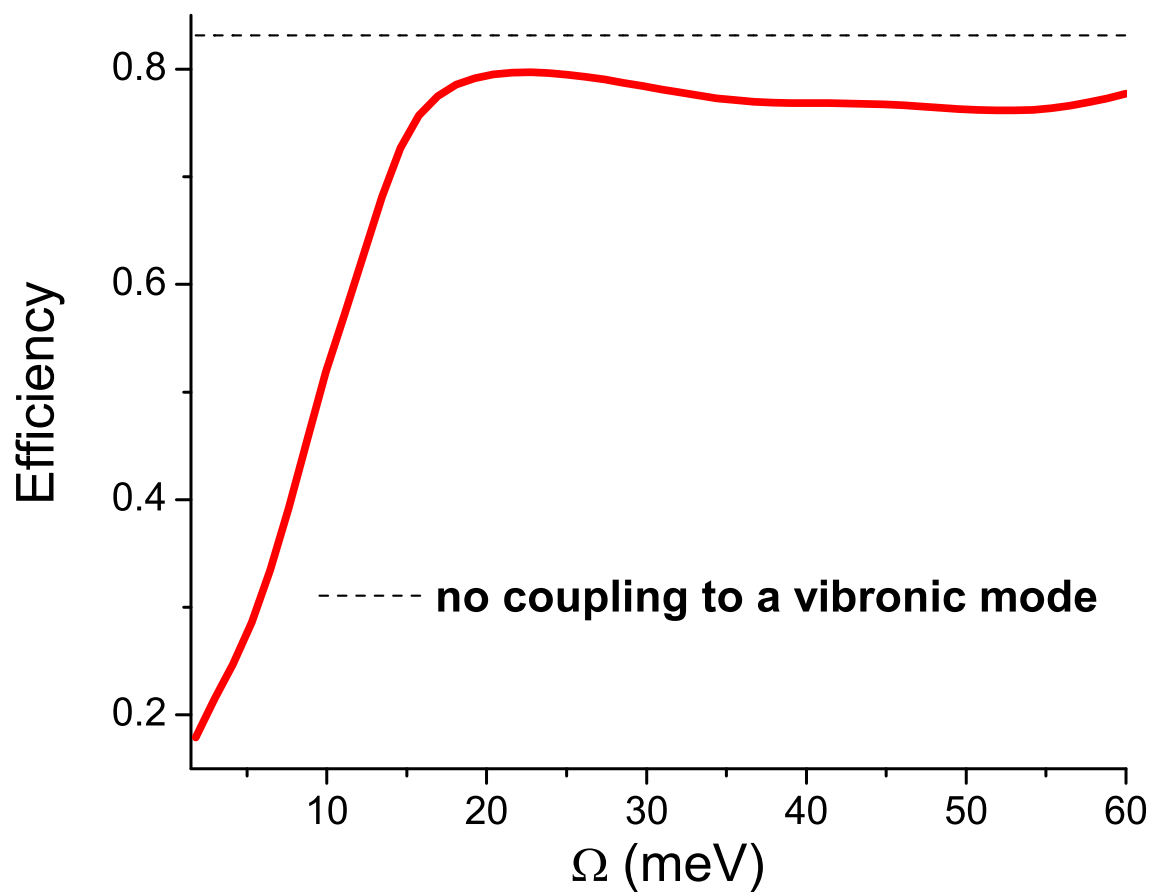


FIG. 3: (Color online) Energy transfer efficiency as a function of the vibronic mode frequency Ω .

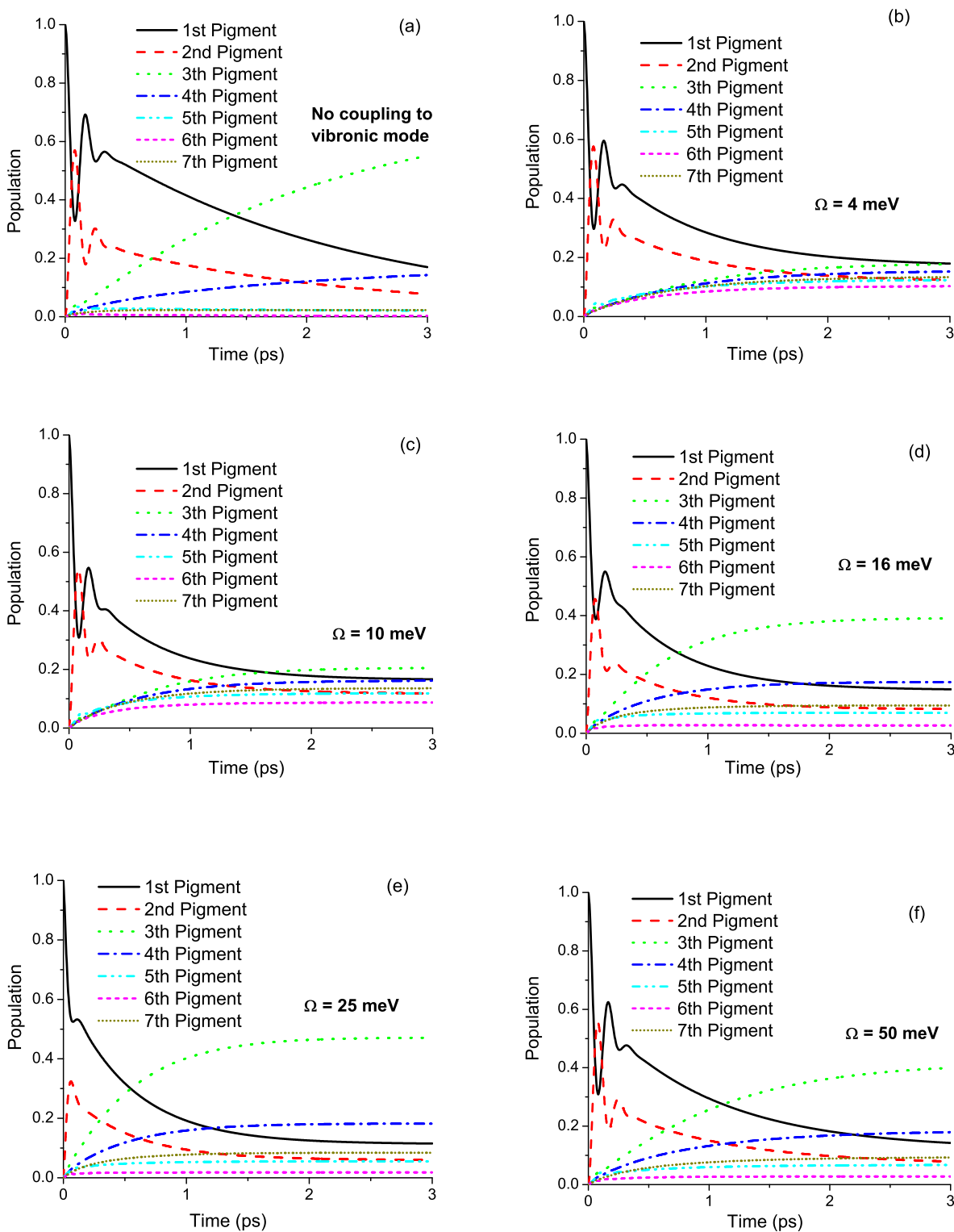


FIG. 4: (Color online) Time dependencies of the pigment populations for various frequencies of the vibronic mode.

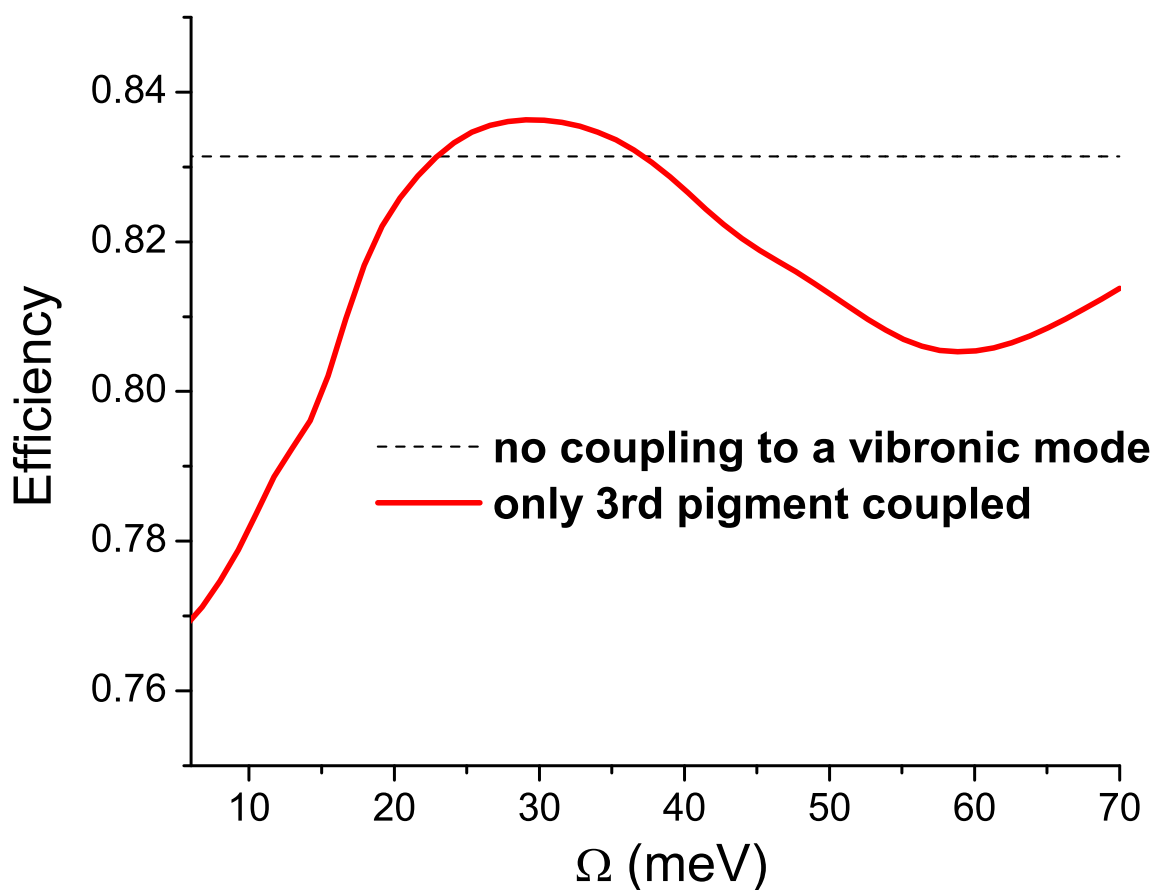


FIG. 5: (Color online) Energy transfer efficiency as a function of the frequency Ω of the vibronic mode coupled only to the third pigment.

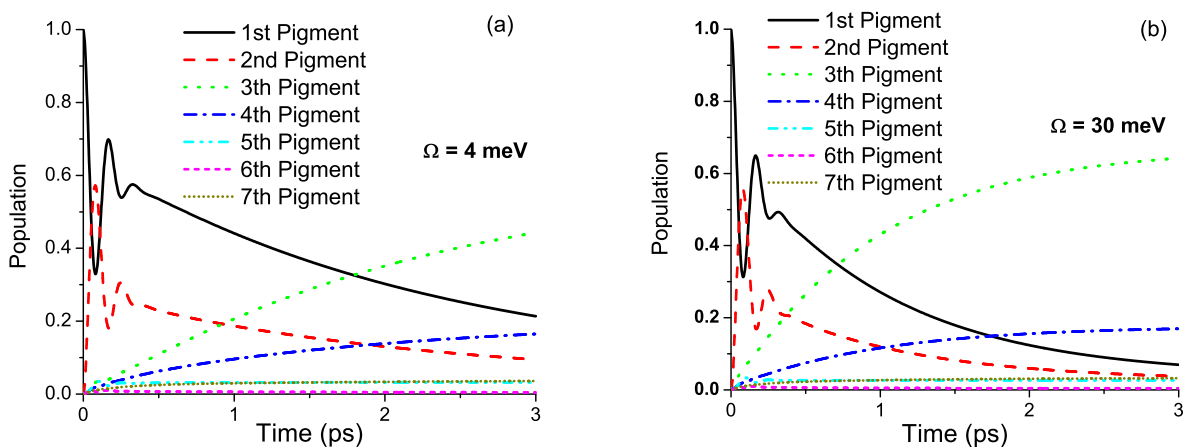


FIG. 6: (Color online) Time dependencies of the pigment populations for various frequencies of the vibronic mode coupled only to the third pigment.